SUPPLEMENTAL DATA

The structural model of the human NHE1 is available at:
http://bioinfo.tau.ac.il/%7Emeytal/index_files/NHE/NHE1.pdb

SUPPLEMENTAL METHODS

Classification and Nomenclature of Na^+/H^+ transporters

NHE1 and EcNhaA belong to two different protein families

NHE1 is a part of the CPA family - TCDB (http://www.tcdb.org/tcdb/) is a database that classifies transport proteins (1). In this database, membrane proteins that transport monovalent cations in exchange for protons belong to the CPA (Cation:Proton Antiporter (TC#2.A.37)) superfamily (1). They are roughly assigned to three families: CPA1 (TC#2.A.36), CPA2 (TC#2.A.37), and the Na^+-transporting carboxylic acid decarboxylase (NaT-DC) family (TC#3.B.1).

The CPA1 and CPA2 families contain exchangers from bacteria, archaea, and eukaryotes. Members of the CPA1 family mostly catalyze Na^+:H^+ exchange, although some might also transport Li^+ or even Ca^{+2} instead of Na^+ (1). The CPA1 family includes the functionally characterized mammalian Na^+/H^+ exchanger (NHE) isoforms, also referred to as the solute carrier 9A (SLC9A) by the HUGO nomenclature (2) (http://www.gene.ucl.ac.uk/nomenclature), and the plant and yeast NHX transporters. Members of the CPA2 family catalyze both K^+/H^+ and Na^+/H^+ antiport, as well as K^+ uniport, and include the KefB/KefC K^+ efflux proteins of *E. coli* that are responsible for glutathione-gated K^+ efflux (1). Members of the NaT-DC family are so far known to contain only bacterial proteins. They export Na^+ from the cell using the energy from decarboxylation of a carboxylic acid substrate.

EcNhaA is a part of the NhaA Na^+:H^+ antiporter family - EcNhaA (the main Na^+/H^+ antiporter in *Escherichia coli*) is classified in TCDB as a unique family called the NhaA Na^+:H^+ antiporter (NhaA) family (TC#2.A.33).

NHE1 and EcNhaA belong to the same superfamily of transporters

Pfam is a comprehensive database for protein domains and families. Protein families that have arisen from a single evolutionary origin are clustered in clans. The CPA1 and CPA2 families (that include NHE1), the K^+ transporter (Trk) family and the NhaA family (that include EcNhaA) are classified into one Pfam clan (the CPA/AT clan) along with proteins that are involved in sodium transport and other proteins of unknown function (3). Pfam divides this clan into 10 different families. The sodium/hydrogen exchanger family (Pfam accession no. PF00999) includes proteins from the CPA1 and CPA2 TCDB families. EcNhaA belongs to a different Pfam family, the Na^+/H^+ antiporter 1 family (Pfam accession no. PF06965), which includes only bacterial proteins.

Evolutionary Conservation Analysis of the NhaA Na^+/H^+ Antiporter Family

The Pfam (4) alignment for the NhaA Na^+/H^+ antiporter 1 family (Pfam accession no. PF06965), comprising 198 sequences, was taken as the initial set of homologous sequences. Redundant (>95% sequence identity) and fragmented sequences were discarded. This intermediate multiple sequence alignment (MSA) of 136 sequences was used to generate a Hidden Markov Model (5), which was subsequently utilized to collect homologous sequences from the UNIPROT database (6). Full-length sequences of these proteins were aligned using the MUSCLE program (7). The N- and C-terminal positions of the alignments were then cut to fit the sequence of EcNhaA (residues 1–388) (SwissProt entry: NHAA_ECOLI). Redundant (>95% sequence identity) and fragmented sequences, sequence variants, and mutants were discarded. Also discarded were proteins that were sequenced by the Whole-genome Shotgun (WGS) project and are therefore considered as preliminary data. The resultant MSA contained 94 sequences of bacterial proteins.

Based on the 94-sequence MSA, evolutionary conservation scores were calculated using a Bayesian method (8) and projected onto the 3D structure of EcNhaA (PDB entry 1ZCD; (9)) using the ConSurf web server (http://consurf.tau.ac.il/) (10).

Evolutionary Conservation Analysis of NHE1-related Na^+/H^+ Exchangers

The ConSeq web server (http://conseq.bioinfo.tau.ac.il/) (11) was used to generate an initial alignment of Na^+/H^+ exchangers as follows. Human NHE1 (residues 105–505) (SwissProt entry: SL9A1_HUMAN) was used as a query sequence to collect homologous sequences from the UNIPROT database (6) using PSI-BLAST (12). The resulting 216 sequences were aligned using MUSCLE (7) with default parameters. Redundant (>95% sequence identity) and fragmented sequences were discarded. The resultant intermediate MSA of 151 sequences was used to generate a Hidden Markov Model (5), which was subsequently utilized to collect remote homologous sequences from the UNIPROT database (6) that were aligned using MUSCLE (7). From the 516 hits found, redundant (>95% sequence identity) and fragmented sequences, sequence variants, and mutants were discarded along with sequences that included irregular characters or ones that were sequenced by WGS project. We then limited the boundaries of the MSA to positions corresponding to residues 126–505 of NHE1, which corresponds to our 3D model of NHE1 described in the main text. The final alignment of 305 proteins from all kingdoms was exclusive to Na^+/H^+ exchangers related to NHE1 and highly reliable to infer position-specific evolutionary information for this transporter.

Based on the 305-sequence MSA, evolutionary conservation scores were calculated using a Bayesian method (8), and, using the ConSurf web-server (http://consurf.tau.ac.il/) (10), were projected onto the 3D model of NHE1 described below.

Identifying the Fold of Eukaryotic Na^+/H^+ Exchangers

Neither the search performed with PSI-BLAST nor the Hidden Markov Model built for NHE1-related Na^+/H^+ exchangers could detect sequences from the prokaryotic NhaA Na^+/H^+ antiporter family, probably because of low sequence similarity. Therefore, to detect those protein structures most likely to possess a similar fold to that of eukaryotic Na^+/H^+ exchangers, we used profile-to-profile alignments implemented in the FFAS03 server (13). The sequences of both human NHE1 (SwissProt entry: SL9A1_HUMAN) and the yeast Na^+/H^+ transporter sod2 (SwissProt entry: NAH_SCHPO) were used as queries. In both cases, EcNhaA was the closest homologue whose 3D structure is known.

Pairwise Sequence Alignment between Human NHE1 and EcNhaA

Generally, and in particular when the sequence homology is low, the use of MSAs to deduce a particular alignment between two sequences produces a more accurate result than the use of a simple pairwise alignment (14-16). Moreover, it was previously shown that construction of alignments using sequence profiles and Hidden Markov Models (5) results in a more accurate match than using standard sequence-based alignments (16-19). The Pfam database (4) provides state-of-the-art Hidden Markov Model-based alignments for protein domains that are predicted to arise from a single evolutionary origin, referred to as clans (3). We therefore used the Pfam's MSA for the clan comprising both EcNhaA and NHE1, and extracted 107 sequences including the bacterial NhaA Na^+/H^+ antiporter 1 family (22 sequences including EcNhaA) and the CPA Na^+/H^+ exchanger family (85 sequences including NHE1). The alignment was also recalculated using MUSCLE (7) to provide an additional alignment method, thereby substantiating the alignment's accuracy. Two pairwise sequence alignment between human NHE1 (SwissProt entry: SL9A1_HUMAN) and EcNhaA (SwissProt entry: NHAA_ECOLI) were directly deduced from the MSAs constructed by Pfam or MUSCLE, as described above. Gaps in corresponding positions were eliminated. Because both alignments yielded similar results, we made no further use of the MUSCLE alignment.

The FFAS03 server applies profile-to-profile alignments and a fold recognition algorithm to detect and align structurally determined proteins to a given sequence (13). As mentioned above, this method detected EcNhaA as the closest structurally determined homologue to NHE1. We therefore used the resulting sequence alignment between these proteins as an additional pairwise alignment.

The HMAP server (15) offers an additional state-of-the-art approach, which we used to calculate the alignment between NHE1 and EcNhaA. HMAP stands for 'hybrid multidimensional alignment of profiles'. This approach combines information on sequence and structure (including secondary and tertiary structures) in order to align remote homologous sequences as accurately as possible (15,17,18). Human NHE1 (SwissProt entry:

SL9A1_HUMAN) was used as the query sequence and EcNhaA (PDB entry: 1ZCD (9)) as the template structure with default parameters to generate an additional pairwise alignment.

Experimental Procedures

Bacterial Strains and Culture Conditions **-** EP432 is an *Escherichia coli* K-12 derivative, which is *mel*BLid, Δ*nha*A1::*kan*, Δ*nha*B1::*cat*, Δ*lac*ZY, thr1 (20). Cells were grown either in L broth (LB) or in modified L broth (LBK (21)).

Plasmids - Plasmid pAXH (previously called pYG10), a pET20b (Novagen) derivative, encodes His-tagged NhaA (22). pCL-AXH, a derivative of pAXH, encodes a His-tagged CL-NhaA (22). pCL-AXH2, a derivative of pCL-AXH, lacks a BglII site at position 3382 (23). pCL-AXH3, a derivative of pCL-AXH2, contains a BstXI silent site at position 248 in *nha*A.

Site-Directed Mutagenesis - Site-directed mutagenesis was conducted according to a PCR-based protocol (24) or DpnI-mediated site-directed mutagenesis (25). For Cys-replacement of W62C, F71C, F72C and G76C and N64C, we used pCL-AXH3 as a template. Mutations H225R and H225C have been previously described (26).

Isolation of Membrane Vesicles and Assay of Na^+/H^+ Antiporter Activity - EP432 cells transformed with the relevant plasmids were grown, and everted vesicles were prepared and used to determine the Na^+/H^+ or Li^+/H^+ antiporter activity as described (27,28). Assay of antiporter activity was based on measurement of the Na^+- or Li^+-induced changes in ΔpH, as measured by acridine orange, a fluorescent probe of ΔpH. The fluorescence assay was performed with 2.5 ml of reaction mixture containing 50−100 μg of membrane protein, 0.5 μM acridine orange, 150 mM KCl, 50 mM BTP, and 5 mM $MgCl_2$, and the pH was titrated with HCl. After energization with D-lactate (2 mM), quenching of the fluorescence was allowed to achieve a steady state, and then Na^+ or Li^+ was added. Reversal of the fluorescence level (dequenching) indicates that protons are exiting the vesicles in antiport with Na^+ or Li^+. As previously shown, the end level of dequenching provides a good estimate of the antiporter activity (29) and the ion concentration that yields half-maximal dequenching gives a good estimate of the apparent K_M of the antiporter (29,30). The apparent K_M for Li^+ of EcNhaA is 10-fold lower than that for Na^+ (0.02 mM and 0.2 mM at pH 8.5, respectively). The Na^+/H^+ or Li^+/H^+ antiporter activity was measured with 5 times the concentration of the apparent K_M.

SUPPLEMENTAL TEXT

The Evolutionary Conservation Analyses of the Na^+/H^+ Exchanger family vs. NhaA Na^+/H^+ Antiporter Family

We emphasize that the evolutionary conservation analyses presented in the main text for NHE1 and EcNhaA are based on two distinct alignment sets. While the NhaA Na^+/H^+ antiporter family comprises only protein orthologs from bacteria, the Na^+/H^+ exchanger family is comprised of diverse proteins from prokaryotes, archaea and eukaryotes. Accordingly, the evolutionary conservation analysis of the Na^+/H^+ exchangers represents a more divergent alignment (average sequence identity = 22%) than the one constructed for the NhaA Na^+/H^+ antiporters (average sequence identity = 39%). As the sequences are evolutionarily close, highly conserved residues are more frequent among the NhaA Na^+/H^+ antiporter family with respect to NHE1-related Na^+/H^+ exchangers, as depicted in Figure 3 (main text). Nevertheless, the general trend of the evolutionary conservation analyses projected on both EcNhaA and NHE1 is highly similar.

Mutagenesis of Eukaryotic Na^+/H^+ Exchangers

When analyzing the effects of mutations (as in Tables 1S and 2S), it should be noted that the experimental data indicating the importance of specific residues for the proteins' function should be interpreted with caution. When analyzing the effect of a specific substitution it is necessary to examine various aspects, such as subcellular localization, activity, and—in the case of pH-sensitive transporters—the activity at different pH levels. For example, some mutations resulted in inactive protein at the native active pH value and were therefore considered damaging to ion-translocation. Testing over a broader pH range indicated, however, that the effect of the mutations was reflected in shifting the pH range in which the

protein is active, with no effect on the translocation process. Such residues are considered to be important for the mechanism of pH regulation, but not for ion translocation. Another example of possibly misleading results is given by the C477S, C8R, and C8S NHE1 mutants, which cause loss of activity (31) (Table 1S). Detailed examination showed that these mutants do not reach the plasma membrane and remain trapped inside the cell. The small amounts of protein that do reach the membrane are still active (31). Thus, despite the deleterious effect of the mutations, we do not consider such residues to play a key role in the protein's function because they are not involved in the ion-translocation or pH-regulation mechanisms. Accordingly, these residues are classified as nonessential.

The membrane-topology of our model vs. that of Wakabayashi and co-workers (32)

The two membrane-topologies were based on completely different approaches. Thus, it is encouraging that 9 out of 12 TM segments overlap. The Wakabayashi model was based on hydrophobicity scales and assessed by cysteine-accessibility experiments. Our topology mostly agrees with Wakabayashi's experimental findings (Fig. 3A), mainly in the extra-cellular loops that contain residues that were shown to be accessible to external reagents, and within the TM segments that contain inaccessible residues. Wakabayashi's data include many paradoxical findings, i.e., residues that are sequence-neighbors and yet accessible from both sides of the membrane. This could be a result of flexible regions that are involved in cation-translocation, as the authors suggested. The regions showing paradoxical findings are all located in the cytoplasmic side of our model of NHE1, and theoretically, it is possible that the conflicting results are due to troubles with the cytoplasmic accessibility of the cysteine-directed reagents.

The most apparent difference between the two suggested topologies is the structural assignment of the segment between residues 370-402 (TM9 in our model). Wakabayashi's experimental results in this region display some residues that are accessible to external reagents, followed by inaccessible residues and then again by residues accessible to external reagents. One possible solution to this conundrum is the presence of an intra-membranal segment as the authors suggested. Since the cysteine-accessibility analysis is not conclusive (as other NHE1 regions show paradoxical findings), and there are no other indications for the presence of such intra-membranal segment in NHE1, we suggest that structurally-simpler alternatives be considered, especially that the bacretial homologue EcNhaA does not manifest such segment. For example, the accessibility of a cytoplasmic region to external reagents could be the result of this region participating in ion translocation.

The first two TM segments in the Wakabayashi model are hydrophobic stretches and correspondingly were detected as membranal by hydrophobicity scales. Nevertheless, as mentioned in the main text, this region is highly variable amongst the Na^+/H^+ exchanger family, and some homologues lack this segment altogether. Moreover, it was shown that truncation of the first 150aa in NHE1 do not affect activity (33). In EcNhaA, on the other hand, the first two TM segments are important and play a role in regulation (9). The second TM is specifically involved in the formation of the funnels putatively involved in cation-translocation (9). We therefore suggest that, in NHE1, the first two hydrophobic stretches detected by Wakabayashi do not correspond to the first two segments in EcNhaA. One possibility is that NHE1 contains two additional TM segments at the N-terminus comparing to EcNhaA; these segments might be part of the signal peptide that is truncated in the mature protein (34).

Finally, we relate to the discrepancy between the two topologies within residues 331-362. Our model predicts two TM segments in this region (TM7-8), while there is only one segment in the Wakabayashi model. Since Wakabayashi's hydrophobicity-scale-based predictions were restricted to 21 residues for each TM segment assignment, only one segment could be predicted within this region. On the other hand, this segment of 32 amino acids contains many hydrophobic residues along its whole length, and could easily accommodate two shorter segments. Such an outcome could not be predicted using Wakabayashi's approach due to the shortcoming of the computational method, yet concur with our model that is based on the topology of EcNhaA.

3D-location of identical residues between NHE1 and EcNhaA

Our main working hypothesis is that NHE1 and EcNhaA share a similar fold. Thus, a general assumption is that at least some of the identical residues are structurally important, i.e., buried within the protein core and maintaining the architecture. However, it is unclear how many residues are needed for that. The alignment between NHE1 and EcNhaA, presented in Figure 1S, contains 44 identical residues. We analyzed the 3D-location of these residues within the NHE1 model and found that about half are buried in the protein core, i.e., face neighbouring helices (Figure 2SA). The question is does it make sense? Theoretically, it is not trivial to foresee the 3D-location of identical residues between two sequences. For example, proteins that share 80% sequence identity are most likely to share a similar fold. Nevertheless, only a certain percentage of their identical residues are structurally important. Thus, in this case most of the identical residues might not be buried within the protein. So, what is the minimal fraction of identical residues that are needed in order to maintain a fold? 30%, 10% or even 2%? Currently, there is not enough structural information to answer the above question unequivocally, and it will have to wait for the determination of more protein structures. Moreover, in transmembrane proteins, residues facing the lipids bear an evolutionary constraint to be hydrophobic, which might add to the percentage of structurally-irrelevant residues that are identical between two proteins sharing a similar fold. The exact number of residues needed to maintain a fold is probably indefinite and family-specific, thus unknown for families in which only one member has a determined 3D-sturcture. In general, it may be risky to conclude about structurally-important residues based on pair-wise alignment and one has to look at multiple alignments instead. This point is demonstrated below.

The lactose-permease and glycerol-3-phosphate transporter are TM proteins that share a similar structure inspite of low sequence identity of 10%, as we proposed for NHE1 and EcNhaA. The crystal structures of lactose permease (35) (PDB code – 1PV7) and glycerol-3-phosphate transporter (36) (PDB code – 1PW4) display similar fold and belong to the same SCOP superfamily: MFS general substrate transporter. The structures are superposable with an RMSD of 2.08 for 246 Cα atoms. The 43 identical residues are presented in Fig. 3S, and include both buried and solvent-exposed residues. The buried residues (14 in the lactose permease and 16 in the glycerol-3-phosphate transporter structures) comprise only about 35% of the identical residues (less than in the NHE1/EcNhaA pair), suggesting that only few of these residues are needed to determine the general fold.

Another point of view is the interpretation of the information extracted from a pair-wise sequence alignment. It probably does not hold enough information to determine which of the identical residues are indeed functionally or structurally important and which of these residues did not have enough evolutionary time to substitute. By comparing multiple homologous proteins we can extract the important residues; amino acid positions that are conserved in an entire protein family are more likely to play key roles, while other positions, even if they are conserved between two of the family membranes, are probably less important or involved in specific functions. Therefore, we added homologous sequences of human NHE isoforms and bacterial NhaA proteins to the NHE1/EcNhaA pairwise alignment. As more sequences were added to the alignment, the percentage of the identical residues facing the lipids became smaller (Figure 2S). When only 8 total sequences comprised the alignment, all the identical residues were buried in the protein core (Figure 2S J-L).

To conclude, we suggest that the identical residues shared between NHE1, EcNhaA and their homologous are probably important to maintain the fold, and we show that they are indeed buried within the protein core of our model structure. This result farther supports the proposed model-structure.

Methods

The solvent-accessible (or Connolly) surface area of each residue in the model-structure of NHE1, as well as in the structures of the lactose permease and glycerol-3-phosphate transporter, was calculated using the SURFV program with a probe sphere of radius 1.4Å and default parameters (37). The percentage of surface-exposure of each residue in the protein was calculated using the total solvent-accessible area of the residue within the context of a

Gly-X-Gly tripeptide (where X represents each of the 20 amino-acids) as a reference. When the fraction of the surface-exposure was less than 5%, the residue was considered to be buried, and when more than 20%, the residue was considered to be exposed.
Superimposition of the structures of lactose permease (35) (PDB code – 1PV7) and glycerol-3-phosphate transporter (36) (PDB code – 1PW4) was carried out using MultiProt (38).

The pairwise alignment of NHE1 and EcNhaA presented in Figure 1S was used to build a profile, based on which other homologous sequences from human and bacteria were aligned using CLUSALW (39).

SUPPLEMENTAL TABLES

Table 1S. Published Mutations in Human NHE1

Mutations in human NHE1	**Structural location**	**Conservation (1–9: variable-to-conserved) NHE/EcNhaA**	**Equivalent residue in EcNhaA**	**Notes**	**Citation**
Putatively essential residues					
Gly148 (examined in the rat NHE1 – residue G152)	Loop1-2	1/3	Ser31	Moderately important for inhibitor binding. G148A – reduced sensitivity to EIPA by 3- fold.	(40)
Pro153+ Pro154 (examined in the rat NHE1 – Pro157+) Pro158)	Loop1-2	2/1 3/1	Gly36+ Trp36	Moderately important for inhibitor binding. P153S/P154F – reduced sensitivity to EIPA by 7-fold.	(40)
Phe161 (examined also for the hamster NHE1 – F165)	TM2	7/8	Ile63	Important for activity and also for inhibitor binding. Suggested as a pore-lining residue. F161Y – increases the K_i for amiloride by 40-fold and reduces the Na^+ transport rate by 3- to 4-fold. The effect was also shown for F161Y+F164Y (substitutions as in NHE4).	(41,42)

Phe162	TM2	7/9	Asn64	Important for transport and inhibitor binding. F162S – dramatic decrease in affinity for cariporide and amiloride by 1550- and 150-fold, respectively. The mutant also reduces the affinity for sodium.	(43)
+Ile169 +Ile170	TM2	9/9 8/9	Phe71+ Phe72	F162S together with I169S or I170T – Normal cation-binding (reversion phenotype), but still interference with the inhibition by cariporide. F162S/I169S/I170T triple mutant – the affinity to sodium is as for wt (reversion phenotype), low affinity to cariporide, and a 4- to 5-fold increase in its Km for lithium. I169S+I170T – Interference with ion-translocation, but no effect on inhibition by cariporide. I169S alone – No effect. I170T alone – No effect.	

Leu163 (examined also for the hamster NHE1 – L167)	TM2	5/9	Asp65	Important for inhibitor binding. L163F – reduces the effectiveness of EIPA and MPA to block transport by ~30-fold, and that of amiloride by 3-fold. Note: the corresponding residue to NHE1's Leu163 in rabbit NHE2 (Leu143) is also involved in amiloride binding (44).	(40,41)
Pro167	TM2	8/8	Ala69	Important for activity. P167G/C - abolishes NHE activity. P167A - markedly decreases activity. P167G/C/A- expressed at lower levels compared to wt, and a significant portion of P167G and P167C is retained intracellularly.	(45)
Pro168	TM2	7/5	Val70	Important for activity. P168A/C - abolishes activity. P168G - markedly decreases activity. P168 G/C/A -expressed at levels similar to wt and targeted to the plasma membrane.	(45)
Gly174	TM2	8/9	Gly76	Moderately important for inhibitor binding. G174S – shows 3.3-fold decrease in amiloride affinity. G174D – shows 4-fold decrease in amiloride affinity. G174A – no change is amiloride affinity.	(46)

Leu163+ Gly174	TM2	5/9 8/9	Asp65+ Gly76	Important for inhibitor binding. L163F/G174S double mutant – as active as the wt, but reduced affinity for sodium and for amiloride and its derivatives compared to that of the wt. Each of them alone does not affect Na^+ affinity.	(41)
Arg180	TM2	5/9	Glu82	Important for allosteric regulation. R180K – reduces sensitivity to intracellular protons.	(47)
Ile251	Loop 4-5	8/8	Val148	Moderately important for inhibitor binding. I251A – more resistant to EMD87580 by 3-fold compared to wt.	(48)
Leu255	TM5	7/8	Leu152	Important for activity and moderately important for inhibitor binding. L255A - more sensitive to EMD87580 by 2.5-fold. Also show direct effects on activity.	(48)
Ile257	TM5	7/6	Ile154	Important for activity. I257A – shows direct effects on activity.	(48)
Val259	TM5	8/9	Leu156	Important for activity. V259A – shows direct effects on activity.	(48)
Phe260	TM5	8/6	Met157	Important for activity. F260A – shows direct effects on activity.	(48)

Gly261	TM5	9/8	Ala158	Important for activity. G261A – shows direct effects on activity.	(48)
Glu262	TM5	9/8	Leu159	Important for activity. E262Q – abolishes activity. E262D – reduces activity (less than 25% of that of the wt) and also decreases affinity for Li^+. The substitution of aspartate for glutamate, with its smaller side, chain may reduce the ability of the protein to coordinate the smaller lithium ion, while still allowing for coordination of the larger Na^+ ion. E262D/Q – expressed and targeted to the plasma membrane. E262I – abolishes activity; the nature of the defect was not investigated. E262A – low expression and major effects on targeting (found principally in intracellular compartments). However, even after correcting for targeting and expression, the corrected activity of Glu262 was only 52% of control levels, indicating there was still a significant defect in the Na^+/H^+ exchanger activity. Note: the residue that corresponds to E262 in the sod2 transporter from *Schizosaccharomyces pombe* (fission yeast)	(48,50,51)

				(Glu173) is also critical for activity (49).	
Leu265	TM5	8/7	Ile162	Moderately important for inhibitor binding. L265A – more sensitive to EMD87580 by 10-fold.	(48)
Asn266	TM5	9/9	Asp163	Important for activity. N266A – shows direct effects on activity.	(48)
Asp267	TM5	9/9	Asp164	Important for activity. D267N – no activity. D267E – active. Note: the residue that corresponds to E262 in the sod2 transporter from *Schizosaccharomyces pombe* (fission yeast) (Asp178) is also critical for activity (52).	(48,50)
Thr270	TM5	8/9	Ala167	Important for activity. T270A – shows direct effects on activity.	(48)
Val272	TM5	9/4	Ile169	Moderately important for inhibitor binding. V272A - more resistant to EMD87580 by 5-fold. The mutant also shows reduced expression with no effect on activity.	(48)
Leu273	TM5	7/8	Ile170	Moderately important for inhibitor binding. L273A – shows reduced expression, but after correction for protein expression, its activity was greater	(48)

				than that of controls. Also shows increased resistance to EMD87580 by 2.5 fold.	
Arg327	Loop 6-7	4/-	Gap(204-205)	Important for pH regulation. R327E – significantly shifts the pH set point of NHE1 to the acidic side. R327K – no effect.	(47)
Arg330	Loop6-7	6/-	Gap (204-205)	Important for allosteric regulation. E330M – reduces sensitivity to intracellular protons. R330Q – no effect.	(47)
Glu346 (examined also in the rat NHE1 – E350)	Loop 7-8	7/7	Leu220	Important for activity and for inhibitor binding. E346Q – reduces sensitivity to amiloride and EIPA by 20- and 127-fold, respectively, and also reduces the transport rate. E346/D/N – reduces sensitivity to EIPA by ~500- and ~60-fold, respectively, and also reduces the transport rate. E346D – also reduces the affinity for sodium. This residue has no effect on pH regulation.	(40,53)
His349	TM8	5/9	Gly223	Moderately important for inhibitor binding. H349Y/F – increases sensitivity to amiloride by ~2-fold. H349G/L – reduces	(54)

				sensitivity to amiloride by ~2-fold. H349S (mimics NHE3) – practically no effects on amiloride sensitivity. H349G/L/Y/F/S – all as active as the wt, with similar affinities for the cations.	
Gly352 (examined in the rat NHE1 – G356)	TM8	8/8	Ala226	Important for activity and inhibitor binding. G356A – reduces the apparent half-maximal inhibition of NHE1 by amiloride, EIPA and HOE694 by ~5-, 32-, and 342-fold, respectively. G352S – decreases EIPA sensitivity by 72-fold. G352D – decreases EIPA sensitivity by 33-fold. G352S/L/D/K – significantly reduces transport. This residue has no effect on pH regulation. Note: the corresponding residue in NHE3 (A305) is also involved in amiloride binding (40). Also, the corresponding residue in *C. albicans* Cnh1p (Asp267) (55), *S. cerevisiae* Nha1p (Asp267) (56), *Schizosaccharomyces pombe* (Asp267) (49,52), and *Zygosaccharomyces rouxii* Sod2-22p (Asp266) (57) are crucial for function.	(40)

Leu163+ Gly352 (examined in rat NHE1 L167+ G356)	TM2 TM8	5/9 8/8	Asp65 Ala226	Involved in inhibitor-binding. L163F/G352A – shows 164-fold lower affinity for EIPA compared to wt.	(40)
Glu391	TM9	9/7	Leu264	Important for activity. E391Q – activity is greatly reduced, but not abolished. E391D – active. Note: the corresponding residue in In the *Saccharomyces cerevisiae* Nhx1 (Glu355) is also important for activity (58).	(50)
Cys421	TM10	6/9	Leu296	Important for activity. C421S – small decrease in activity, located in the plasma membrane.	(31)
Arg440	Loop10-11	4/6	Lys315	Important for pH regulation. R440C/D/E/H/L – shift the pH set point of NHE1 to the acidic side with no effect on ion translocation.	(59)
Gly455	TM11	8/7	Cys335	Important for pH regulation. G455C/Q/T/V – shift the pH set point of NHE1 to the alkaline side with no effect on ion translocation. The shift grows larger as the residue becomes bulkier, suggesting a steric hindrance.	(59)

Gly456	TM11	9/9	Gly336	Important for pH regulation. G456C – shifts the pH set point of NHE1 to the alkaline side with no eaffect on ion translocation.	(59)
Putatively nonessential residues					
Cys8	N-terminal	-	-	Essential for localization; nonessential for function C8R/S – intracellular localization (Golgi). However, small amounts of antiporter that reach the membrane are active.	(31)
Asn75	N-terminal	-	-	Glycosylation site. N75D – active as the wt.	(60)
Cys113	N-terminal	-	-	C113S – as active as the WT, located in the plasma membrane.	(31)
His120	N-terminal	-	-	H120G – as active as the wt.	(51,54)
Cys133	TM1	7/5	Ile16	C133S – as active as the WT, located in the plasma membrane.	(31)
Pro178	TM2	7/9	Lys80	P178A – as active as the wt, located in the plasma membrane, expressed at levels similar to wt.	(45)
Glu184	Loop 2-3	4/9	Gly86	E184H – as active as the wt.	(47)

				Note: Mutation in the corresponding position in sod2 (His98) also failed to change activity (52,61)	
Cys212	Loop 3-4	2	Gap(116-117)	C212S – located in the plasma membrane.	(31)
Asp238	TM4	9/9	D133	D238N – as active as the wt. Note: the corresponding residue in the sod2 transporter from *Schizosaccharomyces pombe* (fission yeast) (Asp145) is critical for activity (49,52).	(50)
Pro239	TM4	9/9	I134	P239A – as active as the wt. Note: the corresponding residue in the Sod2-22 transporter from *Zygosaccharomyces rouxii* (Pro145) is critical for activity (62).	(50)
Glu248	TM4	6/8	Leu143	E248Q – as active as wt.	(47)
His250	Loop4-5	5/7	Arg147	Preliminary data suggest that it is not involved in exchanger function.	(51,54)
Leu254	TM5	6/7	Ala151	L254A – shows reduced expression but no effect on activity.	(48)
His256	TM5	6/9	Lys153	H256A – shows reduced expression but no effect on activity.	(48)
Ser263	TM5	9/9	Ala160	S263A – as active as the wt.	(50)
Val269	TM5	8/7	Gly166	V269A – active.	(48)

Val271	TM5	8/9	Ile168	V271A – shows reduced expression but no effect on activity.	(48)
His325	Loop6-7	4/-	Gap(204-205)	H325C – as active as the wt.	(51,63)
Ser359	TM8	7/6	Val233	S359A – as active as the wt.	(50)
Asn370	Loop 8-9	6/1	His243	N370D – as active as the wt.	(60)
Ser387+ Ser388	TM9	7/6 6/6	Ala260+ Tyr261	S387A/S388A – as active as the wt.	(50)
Ser390	TM9	8/7	Ile263	S390A – as active as the wt.	(50)
Thr392	TM9	7/9	Pro265	T392V – as active as the wt.	(50)
Ser401	Loop9-10	7/5	Ser275	S401A – as active as the wt.	(50)
Thr402	Loop9-10	6/4	Leu276	T402V – as active as the wt.	(50)
Ser406	Loop9-10	1/2	Thr280	S406A – as active as the wt.	(50)
Asn410	Loop9-10	1/1	Thr285	N410D– as active as the wt.	(60)
Lys438	Loop 10-11	1/6	Arg313	K438E– as active as the wt.	(47)
Lys443	Loop 10-11	1/1	His318	K443E– as active as the wt.	(47)
Cys477	Loop 11-12	6/2	D354	Essential for localization; nonessential for function. C477S – intracellular localization (Golgi). However, small amounts of antiporter that reach the membrane are active.	(31)

Table 1S: The mutations are divided into putatively essential and nonessential sites. The locations of the mutations on the predicted topology suggested in this paper and their corresponding numbers in EcNhaA are indicated. Conservation scores for NHE1 and EcNhaA are according to the ConSurf 1–9 (variable-to-conserved) scale, calculated using 305 NHE1-

related Na^+/H^+ exchanger homologous sequences or 94 bacterial NhaA Na^+/H^+ antiporters, respectively, as described in Methods. EMD87580 is an amiloride analog.
MPA: N^5-methyl-N^5-propylamiloride; EIPA: 5-(*N*-ethyl-*N*-isopropyl) amiloride.

Table 2S. Published Mutations in Eukaryotic Na^+/H^+ Exchangers

Mutations	**Structural location**	**Conservation (1–9: variable-to-conserved) NHE/EcNhaA**	**Corresponding residue in NHE1/EcNhaA**	**Notes**	**Citation**
Putatively essential residues					
Leu143 In rabbit NHE2 (SL9A2_RABIT)	TM2	5/9	Leu163/Asp65	Important for inhibitor binding. Note: the corresponding position in NHE1 is also involved in amiloride binding (41).	(44)
Thr141 In *Zygosaccharomyces rouxii* Sod2-22p (Q9UUT4_ZYGRO)	TM4	8/7	Ser235 /Ala130	Important for activity. T141S produces a broadened cation selectivity of the antiporter for K^+, in addition to Na^+ and Li^+.	(64)
Asp145 In *Schizosaccharomyces pombe* (fission yeast) sod2 (NAH_SCHPO)	TM 4	9/9	Asp238/ Asp133	Important for activity. Note: in NHE1, mutation of D238N is not crucial for function (50).	(49,52)
P145 In *Zygosaccharomyces rouxii* Sod2-22p (Q9UUT4_ZYGRO)	TM4	9/9	Pro239/Ile134	Important for activity. P145S/T – decreases the antiporter transport activity for both Na^+ and Li^+, yet enables ZrSod2-22p to transport K^+.	(62)

				P145D/K – abolishes activity. P145G – extremely low activity for exchanging Na^+. Note: the corresponding residues in *S. cerevisiae* Nha1 antiporter (Pro146) are also critical for function (62). However, mutation in the equivalent position in NHE1(P239A) is not crucial for activity (50).	
Ser150 In *Zygosaccharomyces rouxii* Sod2-22p (Q9UUT4_ZYGRO)	TM4	8/8	Ala244/ Gly139	Important for activity. S150T produces a broadened cation selectivity of the antiporter for K^+, in addition to Na^+ and Li^+. S150K/R – abolishes activity. S150V/D – no significant change in substrate specificity.	(64)
Glu173 In *Schizosaccharomyces pombe* (fission yeast) sod2 (NAH_SCHPO)	TM 5	9/8	Glu262/Leu159	Important for activity. Note: the corresponding residue in NHE1 is also crucial for function (50).	(49)
Asp178 In *Schizosaccharomyces pombe* (fission yeast) sod2 (NAH_SCHPO)	TM 5	9/9	Asp267/ Asp164	Important for activity. Note: the corresponding residue in NHE1 is also crucial for	(52)

				function (50).	
Asp241 In *Saccharomyces cerevisiae* Nha1p (NAH1_YEAST)	loop 6-7	6/-	Ile326/gap	Intermediate importance for activity. D241N – little effect on Na^+ efflux but significantly reduces K^+ efflux. Note: the corresponding residue in sod2 *Schizosaccharomyces pombe* (Asp241) displays intermediate to insignificant importance for the function of the transporter (49,52,61).	(56)
Asp265 In *Zygosaccharomyces rouxii* Sod2-22p (Q9UUT4_ZYGRO)	TM8	9/9	Ser351/His225	Important for activity. D265V – not active. Note: the corresponding residues in *C. albicans* Cnh1p (Asp266) (55), *S. cerevisiae* Nha1p (Asp266) (56) and *Schizosaccharomyces pombe* (Asp266) (49,52) are also crucial for function.	(57)
Asp266 In *Zygosaccharomyces rouxii* Sod2-22p (Q9UUT4_ZYGRO)	TM8	8/8	Gly352/ Ala226	Important for activity. D266V – not active. Note: the corresponding residues in rat NHE1 (G356) and also in NHE3 (A305) are involved in amiloride binding (40). Also, the corresponding	(57)

				residues in *C. albicans* Cnh1p (Asp267) (55), *S. cerevisiae* Nha1p (Asp267) (56) and *Schizosaccharomyces pombe* (Asp267) (49,52) are crucial for function.	
Glu355 In the *Saccharomyces cerevisiae* Nhx1 (NAH2_YEAST)	TM9	9/7	Glu391/Leu264	Important for activity. E355A – sever impairment of growth. E355Q- partial impairment of growth. Note: the corresponding residue in NHE1 is also important to activity (50).	(58)
His367 In *Schizosaccharomyces pombe* (fission yeast) sod2 (NAH_SCHPO)	TM 11	7/7	Tyr454/Leu334	Important for activity and pH regulation. H367/A- not active. H367D - pH shift to more alkaline pH. Note: the corresponding residue in NHE1 is important for cellular localization (63).	(52,61)
		Putatively nonessential residues			
His67 In *Schizosaccharomyces pombe* (fission yeast) sod2 (NAH_SCHPO)	TM2	5/6	Gln157/Met59	Mutation does not significantly impair proton translocation.	(61)
His98 In *Schizosaccharomyces pombe* (fission yeast) sod2 (NAH_SCHPO)	loop 2-3	4/9	Glu184/Gly86	Mutation does not significantly impair proton translocation. Note: mutation in the corresponding position in NHE1	(52,61)

				also fails to change activity (47).	
His233 In *Schizosaccharomyces pombe* (fission yeast) sod2 (NAH_SCHPO)	loop 6-7	3/-	Phe322/gap	Mutation does not significantly impair proton translocation.	(52,61)
His424 In *Schizosaccharomyces pombe* (fission yeast) sod2 (NAH_SCHPO)	TM12	9/8	Gln495/ Ser372	Mutation does not significantly impair proton translocation.	(61)
His429 In *Schizosaccharomyces pombe* (fission yeast) sod2 (NAH_SCHPO)	TM12	6/1	Arg500/ Tyr377	Mutation does not significantly impair proton translocation.	(61)

Table 2S: The mutations are divided into putatively essential and nonessential sites. The locations of the mutations on the corresponding positions in the predicted topology suggested in this paper for NHE1 and their corresponding numbers in EcNhaA are indicated. Conservation scores are according to the ConSurf 1–9 (variable-to-conserved) scale, calculated using 305 NHE1-related Na^+/H^+ exchanger homologous sequences or 94 bacterial NhaA Na^+/H^+ antiporters, as described in Methods.

SUPPLEMENTAL FIGURES

Figure 1S

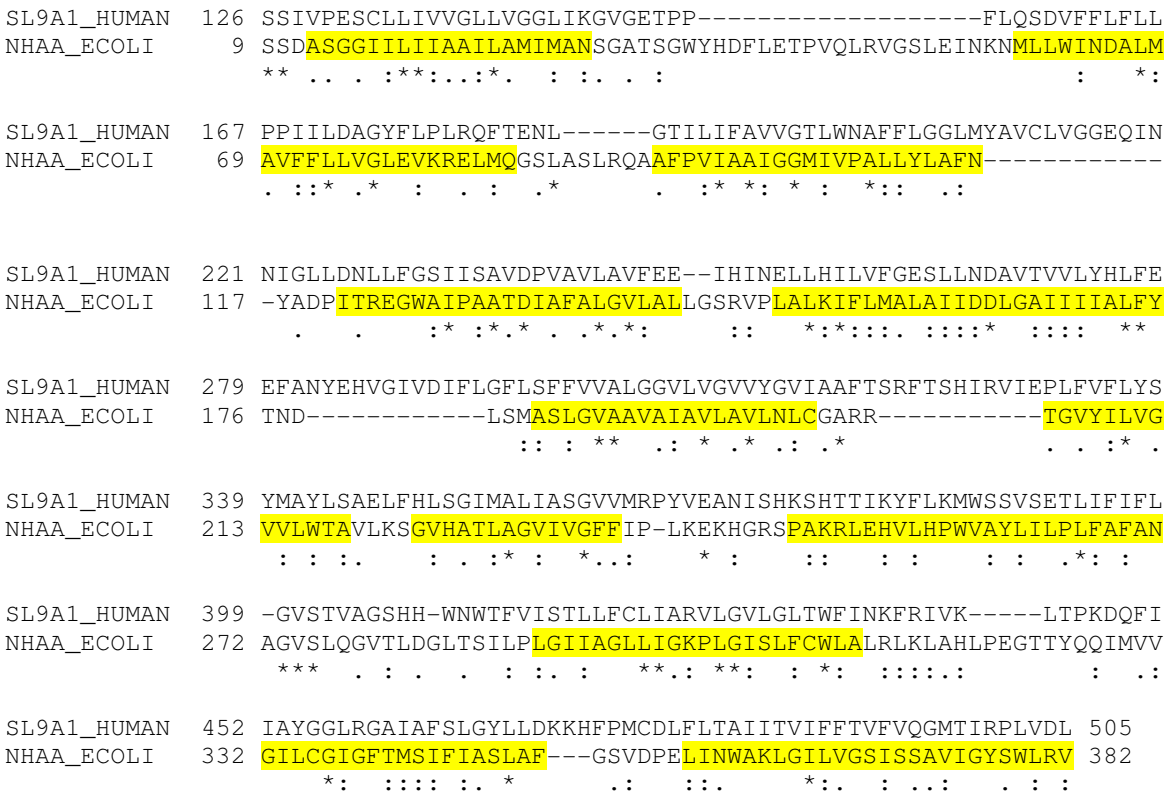

<u>Fig. 1S:</u> Pairwise Alignment between EcNhaA (NHAA_ECOLI) and Human NHE1 (SL9A1_HUMAN).
Construction of the alignment is described in the main text and is based on phylogenetic and structural considerations. The TM segments of EcNhaA, as defined by the crystal structure (9), are highlighted in yellow.

Figure 2S

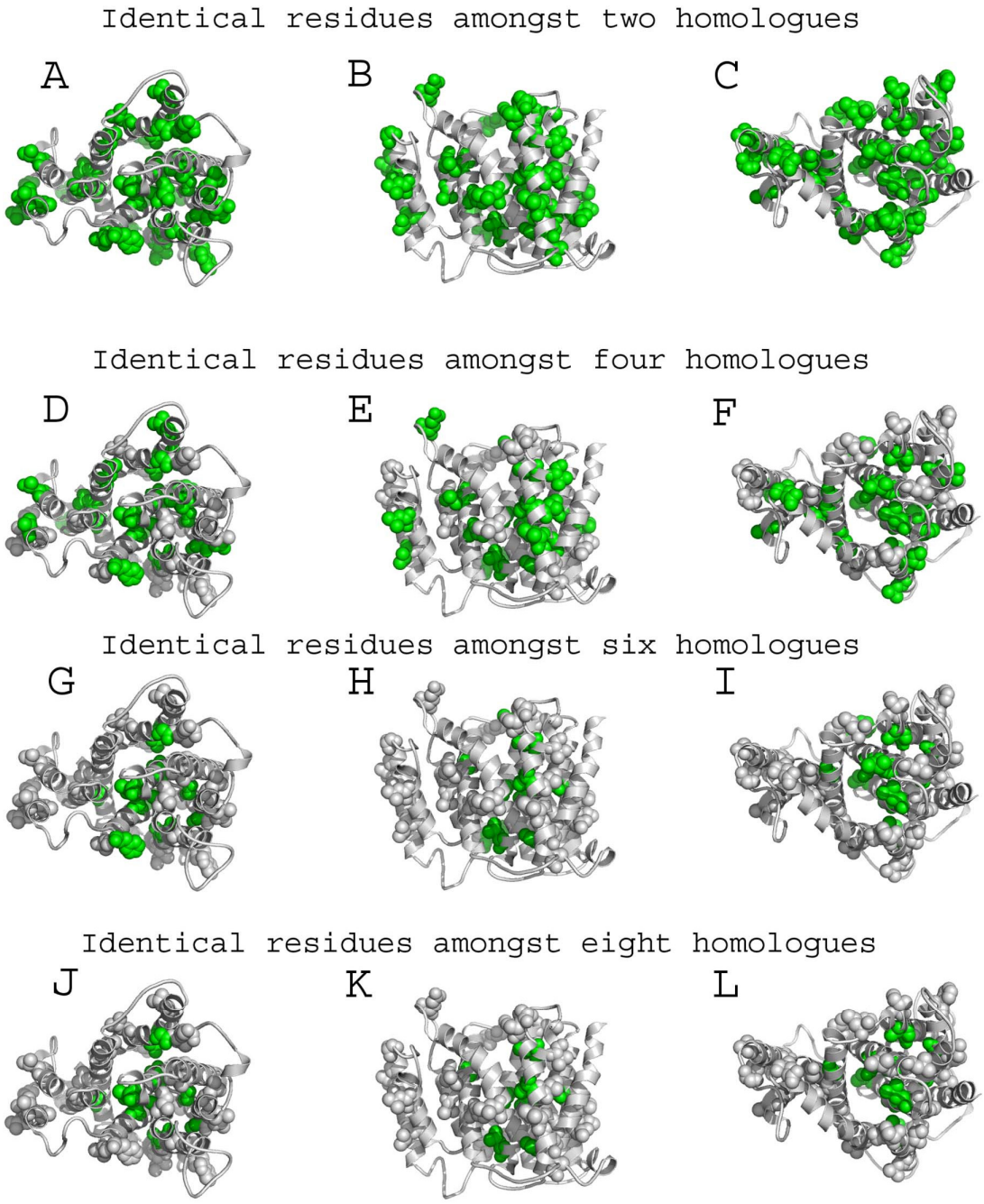

<u>Fig2S</u>: Mapping of Identical Residues between NHE1, EcNhaA and Few of their Homologues on the Model Structure of NHE1.

The 3D model-structure of NHE1 is displayed with gray ribbon and the 44 residues that are identical between NHE1 and EcNhaA, based on the alignment presented in Fig. 1S, are presented using space-filled atoms.

(A-C) The identical residues between NHE1 and EcNhaA are colored green.

(D-F) The 24 residues that are identical between the human NHE1, human NHE2, EcNhaA and NhaA from *Saccharophagus degradans* are colored green.

(G-I) The 14 residues that are identical between the human NHE1, human NHE2, human NHE3, EcNhaA and NhaA from *Saccharophagus degradans* and *Haemophilus influenzae* are colored green.
(J-L) The 12 residues that are identical between the human NHE1, human NHE2, human NHE3, human NHE5, EcNhaA and NhaA from *Saccharophagus degradans*, *Haemophilus influenzae* and *Yersinia frederiksenii* are colored green.
(**A, D, G and J**) A top view from the extracellular side of the membrane. (**B, E, H and K**) A side view parallel to the membrane whereas the intracellular side is facing upward. **(C, F, I and L)** A view from the cytoplasmic side.

Figure 3S

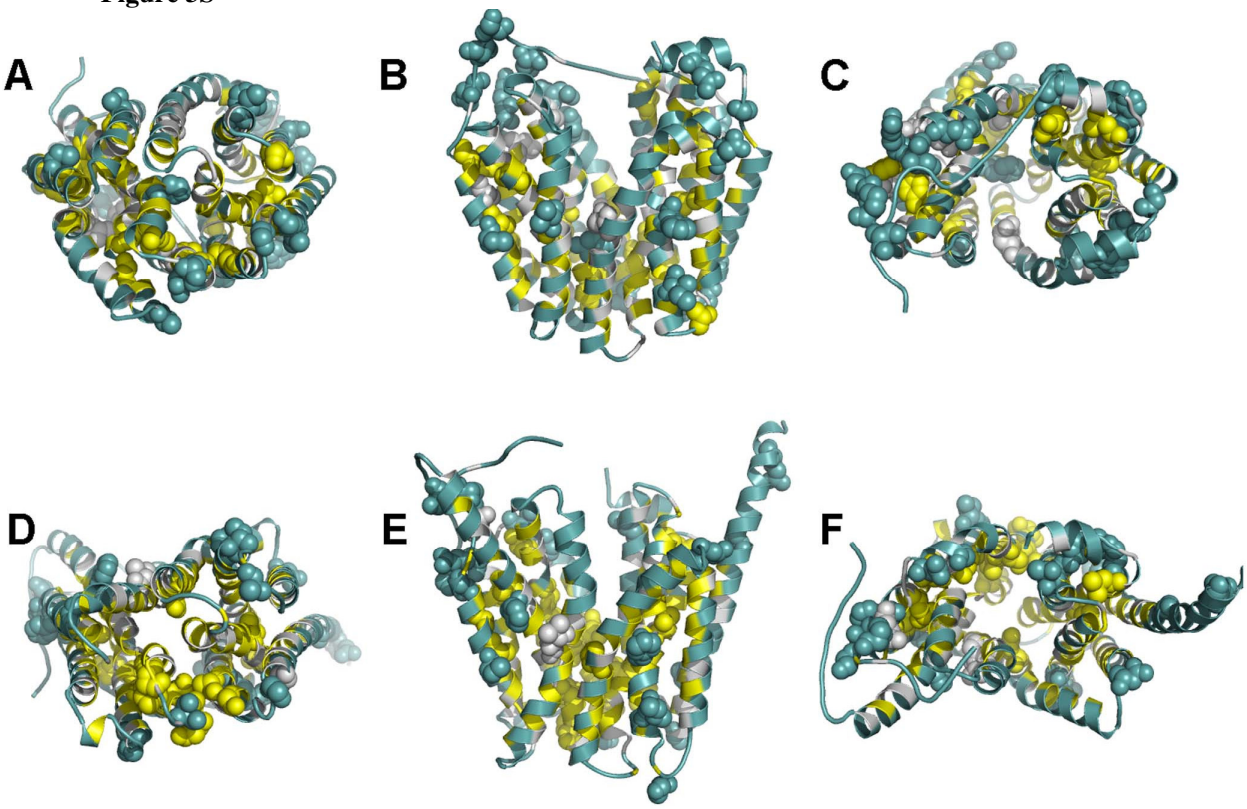

<u>Fig. 3S</u>: Mapping of Identical Residues between Lactose Permease and Glycerol-3-Phosphate Transporter on their Crystal Structures.
The superimposed crystal structure of lactose permease (PDB code – 1PV7) **(A-C)** and glycerol-3-phosphate transporter (PDB code – 1PW4) **(D-F)**, both from E.Coli, are in a gray ribbon representation. Buried and exposed residues are colored yellow and teal, respectively. 43 residues that are identical between the lactose permease and glycerol-3-phosphate transporter are displayed as space-filled models.
(**A and D**) A top view from the extracellular side of the membrane. (**B and E**) A side view parallel to the membrane whereas the intracellular side is facing upward. **(C and F)** A view from the cytoplasmic side.

Figure 4S

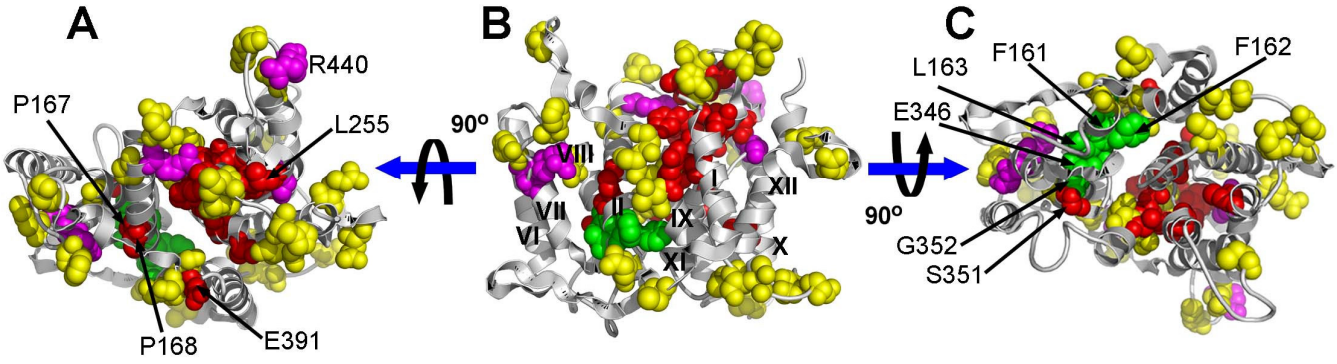

Fig. 4S: Mutagenesis Studies in Eukaryotic Na^+/H^+ Exchangers presented on a Pfam-based Structural Model of NHE1.
The 3D model-structure of NHE1 constructed based on the alignment between NHE1 and EcNhaA derived from the Pfam multiple sequence alignment (see Methods and Figure 2) is displayed with gray ribbon. We note that gaps in the Pfam alignment within TM9 and TM12 resulted in improbable unwinding of these helices. The residues that were mutated are presented using space-filled atoms using colors to represent the experimental outcome: Residues that were implicated in ion-translocation (P167, P168, S235, D238, P239, A244, L255, I257, V259, F260, G261, E262, N266, D267, T270, S351, E391, C421 and Y454) are colored red, residues that are involved in pH regulation (R180, R327, E330, R440, G455 and G456) in magenta, residues comprising the NHE-inhibitors binding-site (F161, F162, L163, E346 and G352) in green, and unessential residues (C133, Q157, P178, E184, C212, E248, H250, L254, H256, S263, V269, V271, F322, H325, S359, N370, S387, S388, S390, T392, S401, T402, S406, N410, K438, K443, C477, Q495 and R500) in yellow (for details see Tables 1S & 2S). (**A**) A top view from the cytoplasmic side of the membrane. (**B**) A side view parallel to the membrane whereas the intracellular side is facing upward; the TM segments are numbered. **(C)** A view from the extracellular side.

SUPPLEMENTAL REFERENCES

1. Chang, A. B., Lin, R., Keith Studley, W., Tran, C. V., and Saier, M. H., Jr. (2004) *Mol. Membr. Biol.* **21**, 171-181
2. Eyre, T. A., Ducluzeau, F., Sneddon, T. P., Povey, S., Bruford, E. A., and Lush, M. J. (2006) *Nucleic Acids Res.* **34**, D319-321
3. Finn, R. D., Mistry, J., Schuster-Bockler, B., Griffiths-Jones, S., Hollich, V., Lassmann, T., Moxon, S., Marshall, M., Khanna, A., Durbin, R., Eddy, S. R., Sonnhammer, E. L. L., and Bateman, A. (2006) *Nucleic Acids Res.* **34**, D247-251
4. Bateman, A., Coin, L., Durbin, R., Finn, R. D., Hollich, V., Griffiths-Jones, S., Khanna, A., Marshall, M., Moxon, S., Sonnhammer, E. L. L., Studholme, D. J., Yeats, C., and Eddy, S. R. (2004) *Nucleic Acids Res.* **32**, D138-141
5. Eddy, S. R. (1996) *Curr. Opin. Struc. Biol.* **6**, 361-365
6. Bairoch, A., Apweiler, R., Wu, C. H., Barker, W. C., Boeckmann, B., Ferro, S., Gasteiger, E., Huang, H., Lopez, R., Magrane, M., Martin, M. J., Natale, D. A., O'Donovan, C., Redaschi, N., and Yeh, L.-S. L. (2005) *Nucleic Acids Res.* **33**, D154-159
7. Edgar, R. C. (2004) *Nucleic Acids Res.* **32**, 1792-1797
8. Mayrose, I., Mitchell, A., and Pupko, T. (2005) *J. Mol. Evol.* **60**, 345-353

9. Hunte, C., Screpanti, E., Venturi, M., Rimon, A., Padan, E., and Michel, H. (2005) *Nature* **435**, 1197-1202
10. Landau, M., Mayrose, I., Rosenberg, Y., Glaser, F., Martz, E., Pupko, T., and Ben-Tal, N. (2005) *Nucleic Acids Res.* **33**, W299-302
11. Berezin, C., Glaser, F., Rosenberg, J., Paz, I., Pupko, T., Fariselli, P., Casadio, R., and Ben-Tal, N. (2004) *Bioinformatics* **20**, 1322-1324
12. Altschul, S., Madden, T., Schaffer, A., Zhang, J., Zhang, Z., Miller, W., and Lipman, D. (1997) *Nucleic Acids Res.* **25**, 3389-3402
13. Jaroszewski, L., Rychlewski, L., Li, Z., Li, W., and Godzik, A. (2005) *Nucleic Acids Res.* **33**, W284-288
14. Petrey, D., Xiang, Z., Tang, C. L., Xie, L., Gimpelev, M., Mitros, T., Soto, C. S., Goldsmith-Fischman, S., Kernytsky, A., Schlessinger, A., Koh, I. Y., Alexov, E., and Honig, B. (2003) *Proteins* **53**, 430-435
15. Tang, C. L., Xie, L., Koh, I. Y., Posy, S., Alexov, E., and Honig, B. (2003) *J. Mol. Biol.* **334**, 1043-1062
16. Rost, B., and O'Donoghue, S. (1997) *Comput. Appl. Biosci.* **13**, 345-356.
17. Elofsson, A. (2002) *Proteins* **46**, 330-339
18. Al-Lazikani, B., Sheinerman, F. B., and Honig, B. (2001) *Proc. Natl. Acad. Sci. U. S. A.* **98**, 14796-14801
19. Jaroszewski, L., Rychlewski, L., and Godzik, A. (2000) *Protein Sci.* **9**, 1487-1496
20. Pinner, E., Kotler, Y., Padan, E., and Schuldiner, S. (1993) *J. Biol. Chem.* **268**, 1729-1734
21. Padan, E., Maisler, N., Taglicht, D., Karpel, R., and Schuldiner, S. (1989) *J. Biol. Chem.* **264**, 20297-20302
22. Olami, Y., Rimon, A., Gerchman, Y., Rothman, A., and Padan, E. (1997) *J. Biol. Chem.* **272**, 1761-1768
23. Galili, L., Rothman, A., Kozachkov, L., Rimon, A., and Padan, E. (2002) *Biochemistry* **41**, 609-617
24. Ho SN, H. H., Horton RM, Pullen JK, Pease LR. (1989) *Gene* **77**, 51-59
25. Fisher, C. L., and Pei, G. K. (1997) *Biotechniques* **23**, 570-574
26. Gerchman, Y., Olami, Y., Rimon, A., Taglicht, D., Schuldiner, S., and Padan, E. (1993) *Proc. Natl. Acad. Sci. USA* **90**, 1212-1216
27. Rosen, B. P. (1986) *Methods Enzymol.* **125**, 328-386
28. Goldberg, E. B., Arbel, T., Chen, J., Karpel, R., Mackie, G. A., Schuldiner, S., and Padan, E. (1987) *Proc. Natl. Acad. Sci. USA* **84**, 2615-2619
29. Schuldiner, S., and Fishkes, H. (1978) *Biochemistry* **17**, 706-711
30. Tsuboi, Y., Inoue, H., Nakamura, N., and Kanazawa, H. (2003) *J. Biol. Chem.* **278**, 21467-21473
31. Wang, H., Singh, D., and Fliegel, L. (1998) *Arch. Biochem. Biophys.* **358**, 116-124
32. Wakabayashi, S., Pang, T., Su, X., and Shigekawa, M. (2000) *J. Biol. Chem.* **275**, 7942-7949
33. Shrode, L. D., Gan, B. S., D'Souza, S. J., Orlowski, J., and Grinstein, S. (1998) *Am. J. Physiol.* **275**, C431-439
34. Sato, Y., and Sakaguchi, M. (2005) *J. Biochem. (Tokyo)* **138**, 425-431
35. Abramson, J., Smirnova, I., Kasho, V., Verner, G., Kaback, H. R., and Iwata, S. (2003) *Science* **301**, 610-615.
36. Huang, Y., Lemieux, M. J., Song, J., Auer, M., and Wang, D. N. (2003) *Science* **301**, 616-620.
37. Sridharan, S., Nicholls, A., and Honig, B. (1992) *Biophys. J.* **61**, A174
38. Shatsky, M., Nussinov, R., and Wolfson, H. J. (2004) *Proteins* **56**, 143-156.
39. Higgins, D. G., Thompson, J. D., and Gibson, T. J. (1996) *Methods Enzymol.* **266**, 383-402.
40. Khadilkar, A., Iannuzzi, P., and Orlowski, J. (2001) *J. Biol. Chem.* **276**, 43792-43800
41. Counillon, L., Franchi, A., and Pouyssegur, J. (1993) *Proc. Natl. Acad. Sci. U. S. A.* **90**, 4508-4512

42. Slepkov, E. R., Rainey, J. K., Li, X., Liu, Y., Cheng, F. J., Lindhout, D. A., Sykes, B. D., and Fliegel, L. (2005) *J. Biol. Chem.* **280**, 17863-17872
43. Touret, N., Poujeol, P., and Counillon, L. (2001) *Biochemistry* **40**, 5095-5101
44. Yun, C. H., Little, P. J., Nath, S. K., Levine, S. A., Pouyssegur, J., Tse, C. M., and Donowitz, M. (1993) *Biochem. Biophys. Res. Commun.* **193**, 532-539
45. Slepkov, E. R., Chow, S., Lemieux, M. J., and Fliegel, L. (2004) *Biochem. J.* **379**, 31-38.
46. Counillon, L., Noel, J., Reithmeier, R. A., and Pouyssegur, J. (1997) *Biochemistry* **36**, 2951-2959
47. Lacroix, J., Poet, M., Maehrel, C., and Counillon, L. (2004) *EMBO Rep* **5**, 91-96
48. Ding, J., Rainey, J. K., Xu, C., Sykes, B. D., and Fliegel, L. (2006) *J. Biol. Chem.* **281**, 29817-29829
49. Fliegel, L. (2005) *Mol. Cell. Biochem.* **268**, 83-92
50. Murtazina, R., Booth, B. J., Bullis, B. L., Singh, D. N., and Fliegel, L. (2001) *Eur. J. Biochem.* **268**, 4674-4685
51. Wiebe, C. A., Dibattista, E. R., and Fliegel, L. (2001) *Biochem. J.* **357**, 1-10
52. Wiebe, C. A., Rieder, C., Young, P. G., Dibrov, P., and Fliegel, L. (2003) *Mol. Cell. Biochem.* **254**, 117-124
53. Noel, J., Germain, D., and Vadnais, J. (2003) *Biochemistry* **42**, 15361-15368
54. Wang, D., Balkovetz, D. F., and Warnock, D. G. (1995) *Am. J. Physiol., Cell Physiol.* **269**, C392-C402
55. Soong, T. W., Yong, T. F., Ramanan, N., and Wang, Y. (2000) *Microbiology* **146**, 1035-1044
56. Simon, E., Clotet, J., Calero, F., Ramos, J., and Arino, J. (2001) *J. Biol. Chem.* **276**, 29740-29747
57. Watanabe, Y., Shimono, Y., Tsuji, H., and Tamai, Y. (2002) *FEMS Microbiol. Lett.* **209**, 39-43
58. Mukherjee, S., Kallay, L., Brett, C. L., and Rao, R. (2006) *Biochem. J.* **398**, 97-105
59. Wakabayashi, S., Hisamitsu, T., Pang, T., and Shigekawa, M. (2003) *J. Biol. Chem.* **278**, 11828-11835
60. Counillon, L., Pouyssegur, J., and Reithmeier, R. A. (1994) *Biochemistry* **33**, 10463-10469
61. Dibrov, P., Young, P. G., and Fliegel, L. (1998) *Biochemistry* **37**, 8282-8288.
62. Kinclova-Zimmermannova, O., Zavrel, M., and Sychrova, H. (2005) *J. Biol. Chem.* **280**, 30638-30647
63. Wakabayashi, S., Pang, T., Su, X., and Shigekawa, M. (2000) *FEBS Lett.* **487**, 257-261
64. Kinclova-Zimmermannova, O., Zavrel, M., and Sychrova, H. (2006) *Mol. Membr. Biol.* **23**, 349-361